

Structural Damages in Syntactic Metal Foams Caused by Monotone or Cyclic Compression

61(2), pp. 146-152, 2017

<https://doi.org/10.3311/PPme.103456>

Creative Commons Attribution 

Bálint Katona^{1*}, Imre Norbert Orbulov^{1,2}

RESEARCH ARTICLE

Received 02 December 2016; accepted after revision 16 December 2016

Abstract

Closed cell, high strength metallic foams, like ceramic hollow spheres filled metal matrix foams are promising materials to build lightweight but high specific strength structural parts. The aim of this study is to investigate the damage of the foam structure during monotone or cyclic compression. The tested metal matrix syntactic foams were produced by inert gas pressure infiltration. Four different alloys as matrix and two different ceramic hollow spheres as filler material were applied. The cylindrical specimens were investigated in quasi-static and high strain rate compression and in cyclic compression. The higher strain rates were ensured by a Split-Hopkinson pressure bar system, while the fatigue tests were performed on a closed loop universal hydraulic testing machine. The failure modes of the foams have explicit differences showing barreling and shearing in the case of quasi-static and high strain rate compression respectively. In the case of the fatigue loading, there was a significant difference between the damage mechanisms of the unalloyed and the Si alloyed matrix syntactic foams. This can be explained by the difference between the yield strength of the matrix material and the ceramics hollow spheres.

Keywords

syntactic foam, metal foam, damage, fatigue, compression

1 Introduction

Metal matrix syntactic foams (MMSFs) can be applied in numerous fields because of their damping effect, low density and high specific strength: parts of aircrafts and vehicles, packing materials, covering or extender of sandwich structures. These materials have high specific compression strength and absorbs high amount of mechanical energy during the compression therefore they can be applied in automotive industry as buffer zones materials. The metal matrix syntactic foams absorb the microwave and the electromagnetic waves as well so they can be also used in electromagnetic shading or shielding.

In most cases the matrix material is aluminium alloy, but steel [1-5], magnesium [6] and titanium [7-9] matrices have also been investigated. The most common filler materials are the ceramic [10-15] or metallic [10] hollow spheres but in order to reduce the costs of the MMSFs perlite [16-18] or pumice [19] are used as well. Mankovits et al. [20-24] and Kozma et al. [25, 26] dealt with the computer tomography and structural reconstruction of MMSFs in order to perform complex finite element analyses with the ultimate goal of mechanical properties prediction. Szalóki et al. has investigated the cutting processes of similar material as described in [27].

Vendra and his research group investigated so called composite metal foams (CMF) which are similar to the MMSFs. They characterized the compressive fatigue properties of the investigated material. The deformation of the CMF samples was divided into three stages: (i) linear increase in strain with fatigue cycles; (ii) minimal strain accumulation in large number of cycles; and (iii) rapid strain accumulation within few cycles resulting in complete failure. Considering the structure of the foams, CMFs underwent a uniform deformation, unlike the regular metal foams, which deformed along collapse bands at weaker sections [28].

Lehmhus et al. investigated powder metallurgical route produced Al6061 alloy foams in as foamed and in precipitation hardened condition under cyclic compression-compression loading. The positive effect of precipitation hardening was only partially experienced in cyclic loading. The phenomenon was explained through the ductile to brittle transition of base material under

¹ Department of Materials Sciences and Engineering
Faculty of Mechanical Engineering
Budapest University of Technology and Economics
H-1111 Budapest, Műegyetem rkp. 3., Hungary

² MTA-BME Research Group for Composite Science and Technology
H-1111, Budapest, Műegyetem rkp. 3., Hungary

* Corresponding author, e-mail: katona@eik.bme.hu

heat treated condition and by the increasing initial crack density due to the heat cycle of precipitation heat treatment [29].

Gupta et al. produced Mg based syntactic foams with extremely low density (0.97 gcm^{-3}), filled with SiC hollow spheres. The peak strength and the elastic energy absorbed up to the peak strength showed an increasing trend by increasing the strain rates (from 1330 to 2300 s^{-1}). The failure at high strain rates was observed to be crushing of the particles, plastic deformation of the matrix, and propagation of cracks along the precipitates on the grain boundaries [30].

Fiedler et al. addressed the dynamic analysis of low cost expanded perlite/aluminium (EP/A356) SFs under dynamic compressive loading conditions. Stresses were found to slightly increase at higher strain rates, indicating positive strain-rate sensitivity. The perlite particles had positive effect on the compression resistance at high loading velocities. A possible explanation was connected to the pressure built-up of the entrapped air within the particles, and the stabilization of adjacent metal struts [31].

The damage of the foam structure in the case of different aluminium matrix - ceramic hollow sphere filled syntactic foams were investigated by Orbulov and Ginszler in compression loading. The process ended at 50% engineering strain. It could be observed that fracture band appeared under $\sim 45^\circ$ as it is expected from the maximum shear stress theory. The shear band was rather wide and very well defined [32].

Zhang et al. investigated different cenospheres filled pure aluminium matrix syntactic metal foams made by squeeze casting technology. They concluded that the deformation behaviour of the syntactic foam from quasi-static to high strain rates shows different features due to the effects of the size of the unit of shear displacement. The unit of shear displacement gets smaller with the increasing strain rates [33].

The aim of this paper is to widen the information about the structural damages in metal matrix foams during monotone and cyclic compression. For the investigations Al99.5, AlSi12, AlMgSi1 and AlCu5 matrix MMSFs with two different filler materials were used.

2 Materials and Methods

The investigated metal matrix syntactic foams were produced by inert gas (Ar) pressure assisted liquid phase infiltration. Table 1 contains the chemical composition of the applied matrix materials.

Table 1 Chemical composition of the matrix materials

| Matrix | Main components (wt%) | | | | | |
|---------|-----------------------|------|-----|-----|-----|-------|
| | Al | Si | Fe | Mg | Cu | other |
| Al99.5 | 99.5 | 0.1 | 0.1 | - | - | 0.3 |
| AlSi12 | 86 | 12.8 | 0.1 | 0.1 | - | 1.0 |
| AlMgSi1 | 97 | 1.1 | 0.5 | 1.1 | - | 0.3 |
| AlCu5 | 95 | - | - | - | 4.5 | 0.5 |

As filler material two different ceramics hollow spheres were used: Globocer-type made by Hollomet GmbH, and SL300-type made by Envinospheres Ltd. Both materials contain 33 wt% Al_2O_3 , 48 wt% amorphous SiO_2 and 19 wt% mullite ($\text{Al}_2\text{O}_3 \cdot \text{SiO}_2$). The volume fraction of the investigated foams was $\sim 64\%$ due to random close packing (RCP) order [34, 35]. The properties of the applied ceramics hollow spheres can be seen in Table 2.

Table 2 The properties of the ceramics hollow spheres

| Filler type | Diameter (μm) | Wall thickness (μm) | Density (gcm^{-3}) |
|-------------|----------------------------|----------------------------------|-------------------------------|
| Globocer | 1444 | 58.0 | 0.816 |
| SL300 | 150 | 6.75 | 0.691 |

From the manufactured MMSF blocks cylindrical specimens were machined for the fatigue and for the compressive (quasi-static and high strain rate) tests.

For the quasi-static and the high strain rate test cylindrical specimens were prepared with diameter of $D=\text{Ø}12.7 \text{ mm}$ and with $H/D=1$ aspect ratio. The quasi-static tests were performed on a MTS 810 type hydraulic materials testing machine at room temperature. For the test a 4 column compression tool were used and the tests were made up to 50% engineering deformation with 0.01 s^{-1} deformation rate. The high strain rate compressions were performed on a Slit-Hopkinson equipment. The transmission bar and the incident bar were made by C350 high strength steel. The length and the diameters of the bars was 1.8 m and $\text{Ø}19.05 \text{ mm}$, respectively. The applied pressure which operated the strike bar with length of 72.2 mm could be adjusted to 138 or 552 kPa. By these two pressure levels 933 and 2629 s^{-1} strain rates could be reached which correspond to a ~ 15 and a $\sim 36 \text{ m/s}$ collision. In these tests MMSF made by Al99.5, AlSi12, AlMgSi1 or AlCu5 matrices and Globocer type filler material were used. All of the specimens were homogenized at 520°C for 30 min. The specimens were cooled in water, and the compression tests were performed immediately after the homogenization process, to avoid any cold aging effect. The AlMgSi1 and AlCu5 specimens were also tested in an aged condition involving a 14 h long aging process at 170°C (followed by water cooling) just after the homogenization stage. The T6 treated specimens were investigated immediately after the aging process.

The fatigue tests were performed on an Instron 8872 servo hydraulic universal testing machine in a two column tool. The diameter of the applied cylindrical specimens was $D=\text{Ø}8.50 \text{ mm}$ and the aspect ratio was $H/D=1.5$. The loading of the specimen was cyclic compression with $R=0.1$ at different load ratios ($k=\sigma_{\text{max}}/\sigma_c$ where σ_{max} is the maximal load of the cycle and σ_c is the compressive strength of the investigated syntactic foams) from 0.7 up to 0.9. The frequency of the fatigue tests was set to $f=10 \text{ Hz}$. As failure criterion a deformation limit was applied,

the specimen considered to be broken if its overall engineering deformation reached $\epsilon=2\%$, but to observe precisely the damage mechanism the tests were continued up to $\epsilon=10\%$ engineering deformation. For the fatigue test four different syntactic foams were used: Al99.5 or AlSi12 matrix filled with Globocer or SL300 ceramics hollow spheres.

The broken specimens which were used for the fatigue or the compression test were embedded in resin. To observe the change of the structure of the foams the samples were grinded to the median plane which were parallel to the load. As last step polishing was used to make the surface fine. We observed the damages caused by monotone or cyclic compression with an Olympus SZX 16 type stereo binocular microscope.

3 Results

3.1 Structural damages in syntactic foams at monotone compression

The quasi-static and high strain rate monotone compression caused damage mechanism was very similar in the case of the different matrix materials (AlSi12 (O), AlCu5 (O), AlCu5 (T6), AlMgSi1 (O) and AlMgSi1 (T6)). Therefore in this study we present only the change of the structure of an Al99.5 matrix Globocer ceramic hollow spheres filled syntactic foam but the conclusions are valid to every investigated syntactic foams as well.

Fig. 1 shows the longitudinal section of a specimen after 2% engineering deformation which was occurred in quasi-static compression. As it can be seen the hollow spheres did not break or crush which means that the plastic deformation of the matrix material caused the overall deformation of the specimen. Fig. 2 shows the section of a specimen after 30% engineering deformation in the case of quasi-static compression. It can be seen the hollow spheres which were in the middle of the material are broken. The barrelling of the specimens can be observed as well. Fig. 3 shows the section of a specimen after 60% engineering deformation in the case of quasi-static compression. As can be seen the hollow spheres were broken in the whole specimen. The collapse of the cells was continuous therefore this material absorbed a high amount of energy during the damage.

With the increasing the strain rate the damage mechanism was changed significantly. Fig. 4a shows a longitudinal section of a specimens after a 933 s^{-1} strain rate compression (split-Hopkinson bar test). The engineering deformation of the foam was $\epsilon=2.45\%$. Compared with the quasi-static compression the high strain rate compression caused the damage of the hollow spheres at $\epsilon=2.45\%$ engineering deformation already. As it can be seen in the wall of the filler parts cracks were formed which are parallel to the direction of the load. Although the hollow spheres were damaged (cracks were occurred) they did not came apart. On the enlarged pictures (Fig. 4b and 4c) cracks can be seen which go in the matrix material and start in the rigid cracks of the hollow spheres. This phenomenon could be caused by the increased gas pressure inside the hollow spheres during the compression.

Rabiei et al. have already observed this in the case of steel hollow spheres filled foam composites [36]. The cracks stop by the matrix material or propagated to the next hollow sphere.

Fig. 5a shows a longitudinal section of a specimen after a 2629 s^{-1} strain rate compression (split-Hopkinson bar test). The engineering deformation of the foam was $\epsilon=8.12\%$. As it can be clearly observed due to the high strain rate compression, the ceramics hollow spheres were broken in the whole specimen, the cells were collapsed and some large cracks parallel to the load were occurred. The specimens were separated 2-3 large pieces. The ceramic hollow spheres came apart which pieces fell out during the grinding and polishing processes. The damage of the filler material can be seen in Fig. 5b and 5c. The cracks between the cells are significantly larger and wider because of the higher inner gas pressure compared to the case of 933 s^{-1} strain rate compression.



Fig. 1 Longitudinal section of an Al99.5-Globocer syntactic foam in the case of quasi-static compression after $\epsilon=2\%$ engineering deformation.

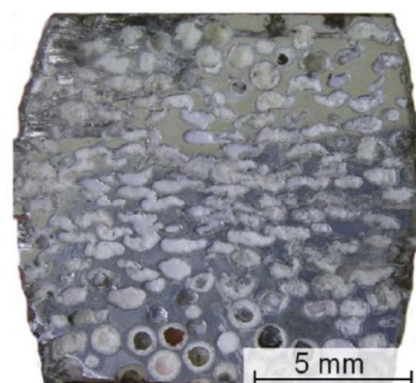


Fig. 2 Longitudinal section of an Al99.5-Globocer syntactic foam in the case of quasi-static compression after $\epsilon=30\%$ engineering deformation.

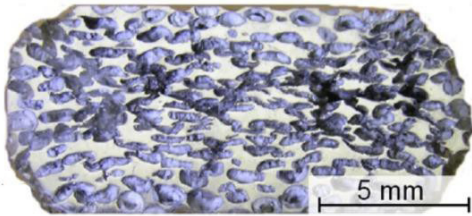


Fig. 3 Longitudinal section of an Al99.5-Globocer syntactic foam in the case of quasi-static compression after $\epsilon=60\%$ engineering deformation.

3.2 Structural damages in syntactic foams due to cyclic compression

In the case of fatigue tests made on different load ratios ($k=\sigma_{\max}/\sigma_c$) the failure mechanism were very similar therefore in this study the characteristic structural damages which were occurred at $k=0.9$ load ratio are presented only.

Fig. 6 shows a longitudinal section of an Al99.5 matrix - SL300 type ceramics hollow spheres filled syntactic foam after the fatigue test. It can be seen the failure of the specimens clearly

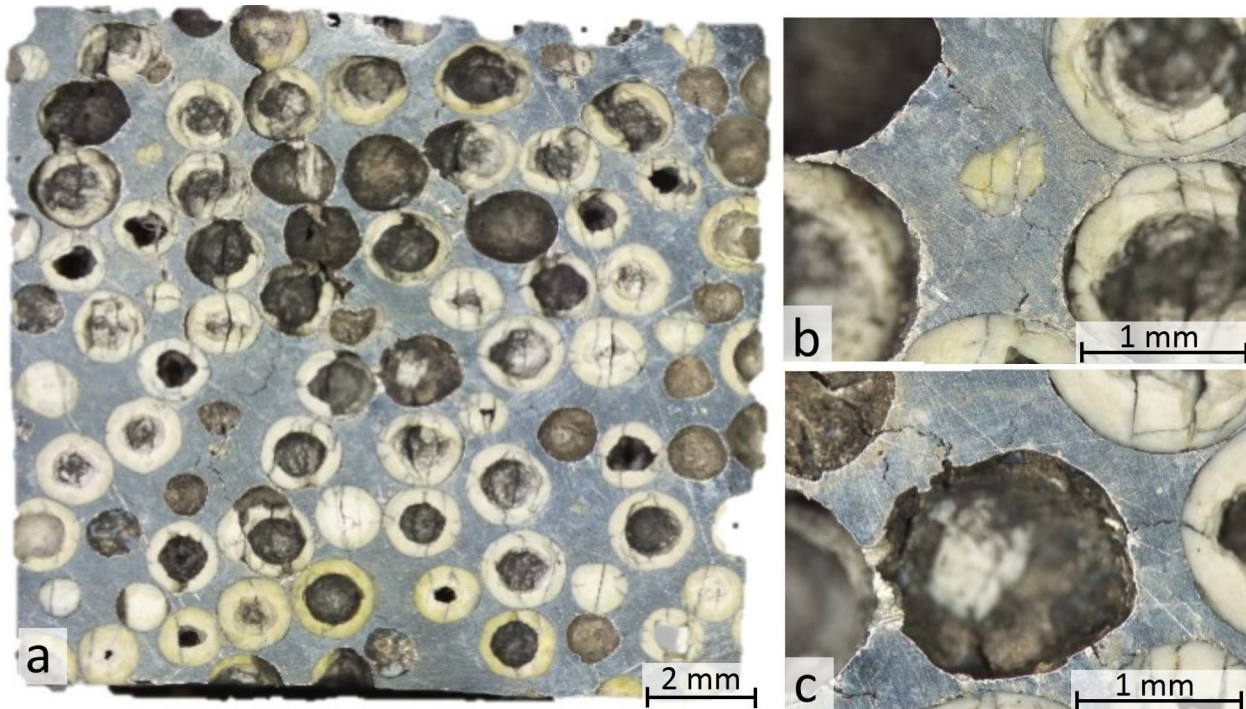


Fig. 4 Longitudinal section of an Al99.5-Globocer syntactic foam in the case of 933 s^{-1} strain rate compression after $\epsilon=2.45\%$ engineering deformation.

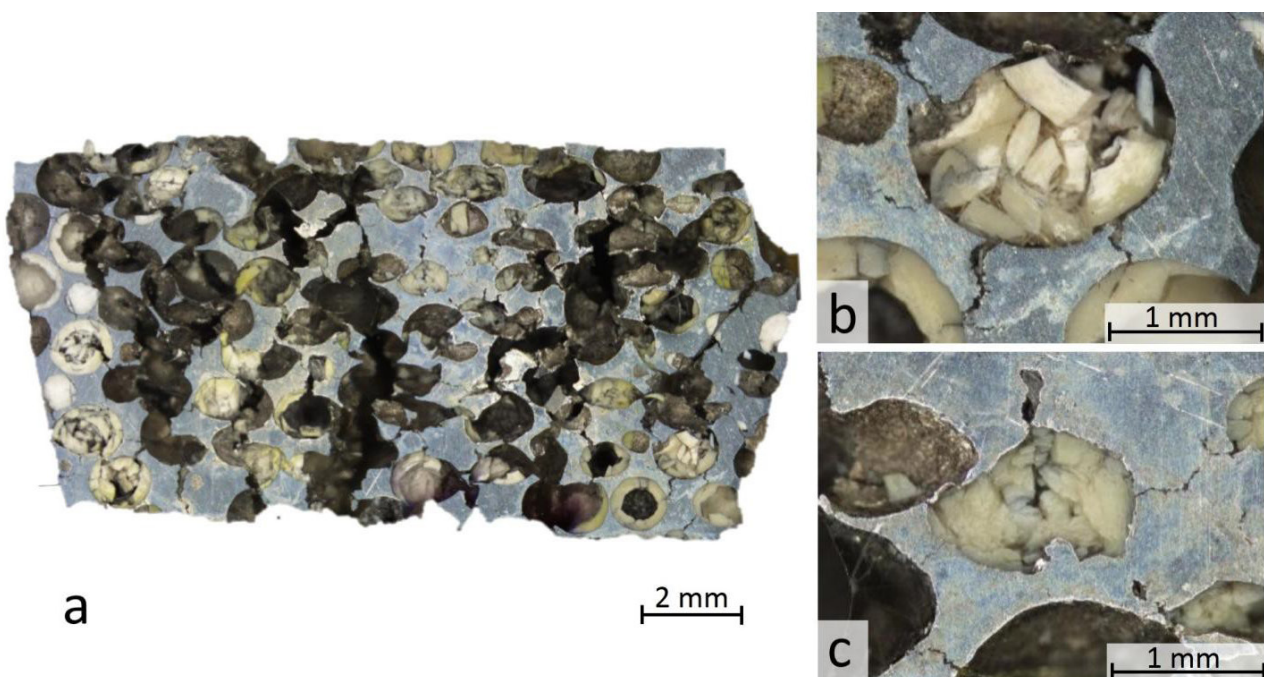


Fig. 5 Longitudinal section of an Al99.5-Globocer syntactic foam in the case of 2629 s^{-1} strain rate compression after $\epsilon=8.12\%$ engineering deformation.

different than by the monotone compression load. The deformation concentrated on a narrow band which inclined 40-45° to the direction of the compression load. In this zone the ceramic hollow spheres were broken, the cells were collapsed and the two parts of the specimens slipped on each other. Far from the damaged band the hollow spheres and the foam structure was remained the original condition.



Fig. 6 Longitudinal section of an Al99.5-SL300 syntactic foam in the case of cyclic compression after $\epsilon=10\%$ engineering deformation.

Fig. 7 shows a longitudinal section of an AlSi12-SL300 syntactic foam after the fatigue test. Similar to the Al99.5- SL300 foam the damage was occurred only at a certain zone of the specimens. In this case the failure concentrated between two compression cones formed on the tool plates. The shape of the failure zone was usually lenticular combined with secondary shear bands at their perimeter. Far from the damaged zones the hollow spheres and the foam structure was remained in the original condition.



Fig. 7 Longitudinal section of an AlSi12-SL300 syntactic foam in the case of cyclic compression after $\epsilon=10\%$ engineering deformation.

The difference between the damage mechanisms can be explained by the difference between the yield strength of the matrix materials and the ceramic hollow spheres. The soft, unalloyed matrix (Al99.5) deformed plastically before the crush of the hollow spheres that resulted in a defined shear band. In the case of harder, Si alloyed matrix material the hollow spheres fractured before the deformation of the matrix material that resulted in a different damage mechanism with the cone-like shear band and the lenticular damage zone.

In the case of larger, Globocer grade ceramics hollow spheres filled syntactic foams the same matrix material depended damage mechanisms were observed.

Fig. 8 shows a longitudinal section of an Al99.5 matrix - Globocer grade ceramic hollow spheres filled syntactic foam after the fatigue test. Similar to the SL300 filled foams during the fatigue test shear band(s) were occurred inclined $\sim 45^\circ$ to the direction of the compression load where the matrix material was deformed plastically, the hollow spheres were broken and the cells were collapsed. Far from these bands the structure was remained the original condition and ready for further loading.



Fig. 8 Longitudinal section of an Al99.5-Globocer syntactic foam in the case of cyclic compression after $\epsilon=10\%$ engineering deformation.

Fig. 9 shows a longitudinal section of an AlSi12-Globocer ceramic hollow spheres filled syntactic foam after the fatigue test. In accordance with the AlSi12-SL300 type syntactic foams the damage mechanism was the same: the failure concentrated between two compression cones formed on the tool plates. The shape of the failure zone was lenticular combined with cone-like shear bands. Far from the damaged zones the hollow spheres and the foam structure was remained unharmed.

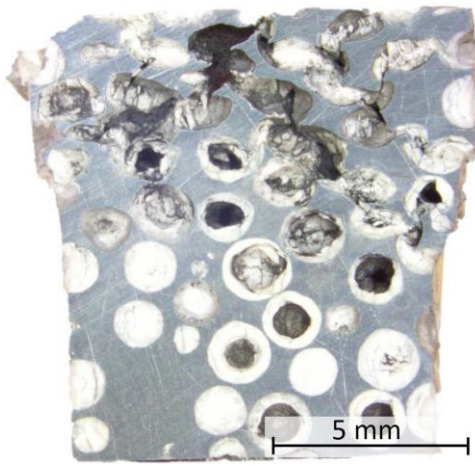


Fig. 9 Longitudinal section of an AlSi12-Globocer syntactic foam in the case of cyclic compression after $\varepsilon=10\%$ engineering deformation.

4 Conclusions

From the above detailed investigations, the following statements can be concluded.

In the case of quasi-static and the high strain rate monotone compression different damage mechanism were observed depending on the strain rate. In the case of quasi-static condition, the matrix material was deformed plastically and the hollow spheres were fractured in the whole specimen. There was no observable difference between the matrix materials. In the case of 933 s^{-1} strain rate compression because of the dynamic impact the damage mechanism was changed: the ceramic hollow spheres were cracked parallel to the direction of the compression load. By the 2629 s^{-1} strain rate compression the hollow spheres fractured and came apart. Some large cracks were observable in the specimen. The collapse of the cells was continuous therefore this material absorbed a high amount of energy during the compression.

In the case of the fatigue tests of the metal matrix syntactic foams a significant difference between the damage mechanisms of the unalloyed and the Si alloyed matrix material syntactic foams was observed. This phenomenon can be explained by the difference between the yield strength of the matrix material and the ceramic hollow spheres. The soft, unalloyed matrix (Al99.5) deformed plastically before the crush of the hollow spheres that resulted in a shear band inclined $\sim 45^\circ$ to the direction of the compressive load. In the case of harder, Si alloyed matrix material the hollow spheres fractured before the deformation of the matrix material that resulted in cone-like shear bands and a lenticular in shape damage zone. Far from the damage zone the foam structure was remained unharmed.

Acknowledgement

This paper was supported by the János Bolyai Research Scholarship of the Hungarian Academy of Sciences.

References

- [1] Castro, G., Nutt, S. R. "Synthesis of syntactic steel foam using gravity-fed infiltration." *Materials Science and Engineering: A*. 553, pp. 89–95. 2015. <https://doi.org/10.1016/j.msea.2012.05.097>
- [2] Castro, G., Nutt, S. R. "Synthesis of syntactic steel foam using mechanical pressure infiltration." *Materials Science and Engineering: A*. 535, pp. 274–280. 2012. <https://doi.org/10.1016/j.msea.2011.12.084>
- [3] Weise, J., Lehmus, D., Baumeister, J., Kun, R., Bayoumi, M., Busse, M. "Production and properties of 316L stainless steel cellular materials and syntactic foams." *Steel Research International*. 85(3), pp. 486–497. 2014. <https://doi.org/10.1002/srin.201300131>
- [4] Luong, D. D., Shunmugasamy, V. C., Gupta, N., Lehmus, D., Weise, J., Baumeister, J. "Quasi-static and high strain rates compressive response of iron and Invar matrix syntactic foams." *Materials & Design*. 66(Part B), pp. 516–531. 2015. <https://doi.org/10.1016/j.matdes.2014.07.030>
- [5] Peroni, L., Scapin, M., Avalle, M., Weise, J., Lehmus, D. "Dynamic mechanical behavior of syntactic iron foams with glass microspheres." *Materials Science and Engineering*. 552, pp. 364–375. 2012. <https://doi.org/10.1016/j.msea.2012.05.053>
- [6] Xia, X., Feng, J., Ding, J., Song, K., Chen, X., Zhao, W., Liao, B., Hur, B. "Fabrication and characterization of closed-cell magnesium-based composite foams." *Materials & Design*. 74, pp. 36–43. 2015. <https://doi.org/10.1016/j.matdes.2015.02.029>
- [7] Mondal, D. P., Datta Majumder, J., Jha, N., Badkul, A., Das, S., Patel, A., Gupta, G. "Titanium-cenosphere syntactic foam made through powder metallurgy route." *Materials & Design*. 34, pp. 82–89. 2012. <https://doi.org/10.1016/j.matdes.2011.07.055>
- [8] Xue, X-B., Wang, L-Q., Wang, M-M., Lü, W-J., Zhang, D. "Manufacturing, compressive behaviour and elastic modulus of Ti matrix syntactic foam fabricated by powder metallurgy." *Transactions of Nonferrous Metals Society of China*. 22, pp. 188–192. 2012. [https://doi.org/10.1016/S1003-6326\(12\)61707-5](https://doi.org/10.1016/S1003-6326(12)61707-5)
- [9] Xue, X-B., Zhao, Y. "Ti matrix syntactic foam fabricated by powder metallurgy: particle breakage and elastic modulus." *JOM*. 63(2), pp. 43–47. 2011. <https://doi.org/10.1007/s11837-011-0027-0>
- [10] Hollomet GmbH. [Online]. Available from: <http://www.hollomet.com> [Accessed: 28th November 2016].
- [11] EnviroSpheres Ltd. [Online]. Available from: <http://www.envirospheres.com> [Accessed: 28th November 2016].
- [12] Sphere Services Inc. [Online]. Available from: <http://www.sphereservices.com> [Accessed: 28th November 2016].
- [13] 3M Company. [Online]. Available from: <http://solutions.3m.com> [Accessed: 28th November 2016].
- [14] Deep Springs Technology. [Online]. Available from: http://teamdst.com/pdf/HollowShells_MTG119-A%20Web.pdf [Accessed: 28th November 2016].
- [15] Ceno Technologies. [Online]. Available from: <http://cenotechnologies.com> [Accessed: 28th November 2016].
- [16] Taherishargh, M., Belova, I. V., Murch, G. E., Fiedler, T. "Low-density expanded perlite–aluminium syntactic foam." *Materials Science and Engineering: A*. 604, pp. 127–134. 2014. <https://doi.org/10.1016/j.msea.2014.03.003>
- [17] Taherishargh, M., Belova, I. V., Murch, G. E., Fiedler, T. "On the mechanical properties of heat-treated expanded perlite–aluminium syntactic foam." *Materials & Design*. 63, pp. 375–383. 2014. <https://doi.org/10.1016/j.matdes.2014.06.019>

- [18] Taherishargh, M., Sulong, M. A., Belova, I.V., Murch, G. E., Fiedler, T. "On the particle size effect in expanded perlite aluminium syntactic foam." *Materials & Design*. 6(Part A), pp. 294–303. 2015.
<https://doi.org/10.1016/j.matdes.2014.10.073>
- [19] Taherishargh, M., Belova, I. V., Murch, G. E., Fiedler, T. "Pumice/aluminium syntactic foam." *Materials Science and Engineering: A*. 635, pp. 102-108. 2015.
<https://doi.org/10.1016/j.msea.2015.03.061>
- [20] Varga, T. A., Mankovits, T. "Fémhab struktúrák elemzése és geometriai modellezése." *International Journal of Engineering and Management Sciences (IJEMS)*. 1(2), pp. 145-152. 2016. (in Hungarian).
<https://doi.org/10.21791/IJEMS.2016.2.19>
- [21] Mankovits, T., Budai, I., Balogh, G., Gábora, A., Kozma, I., Varga, T., Mano, S., Kocsis, I. "Structural analysis and its statistical evaluation of a closed-cell metal foam." *International Review of Applied Sciences And Engineering*. 5(2), pp. 135-143. 2014.
<https://doi.org/10.1556/IRASE.5.2014.2.5>
- [22] Mankovits, T., Budai, I., Balogh, G., Gábora, A., Kozma, I., Varga, T. A., Mano, S., Kocsis, I., Tóth, L. "Structural Modelling Of Closed-Cell Metal Foams." In: Proceedings of the International Scientific Conference on Advances in Mechanical Engineering (ISCAME 2014). (Bodzás, S., Mankovits, T. (eds.)). Debrecen, Hungary, Oct. 08-09, 2014. pp. 70-74.
- [23] Varga, T. A., Kozma, I., Budai, I., Mankovits, T. "Modelling Questions of Metal Foams." In: Proceedings of the 3rd International Scientific Conference on Advances in Mechanical Engineering, (ISCAME 2015). (Bodzás, S., Mankovits, T. (eds.)). 2015. pp. 258-262.
- [24] Varga, T. A., Kapusi, T. "Digital image analysis of metal foam specimens." In: Proceedings of the 4th International Scientific Conference on Advances in Mechanical Engineering, (ISCAME 2016). (Bodzás, S., Mankovits, T. (eds.)). 2016. pp. 584-587.
- [25] Kozma, I., Zsoldos, I., Dorogi, G., Papp, S. "Application of Computed Tomography in Structure Analyses of Metal Matrix Syntactic Foams." *International Journal of Computer Theory and Engineering*. 7(5), pp. 379-382. 2015.
<https://doi.org/10.7763/IJCTE.2015.V7.989>
- [26] Kozma, I., Zsoldos, I., Dorogi, G., Papp, S. "Computer tomography based reconstruction of metal matrix syntactic foams." *Periodica Polytechnica Mechanical Engineering*. 58(2), pp. 87-91. 2014.
<https://doi.org/10.3311/PPme.7337>
- [27] Szalóki, I., Sipos, S., Viharos, J. Z. "Aluminum-Based MMC Machining with Carbide Cutting Tool." *Key Engineering Materials*. 686, pp. 149-154. 2014.
<https://doi.org/10.4028/www.scientific.net/KEM.686.149>
- [28] Vendra, L., Neville, B., Rabiei, A. "Fatigue in aluminum– steel and steel–steel composite foams." *Materials Science and Engineering: A*. 517(1-2), pp. 146–153. 2009.
<https://doi.org/10.1016/j.msea.2009.03.075>
- [29] Lehmus, D., Marschner, C., Banhart, J., Bomas, H. "Influence of heat treatment on compression fatigue of aluminium foams." *Journal of Materials Science*. 37(16), pp. 3447-3451. 2002.
<https://doi.org/10.1023/A:1016506905271>
- [30] Anantharaman, H., Shunmugasamy, V. C., Strbik, III, O. M., Gupta, N., Cho, K. "Dynamic properties of silicon carbide hollow particle filled magnesium alloy (AZ91D) matrix syntactic foams." *International Journal of Impact Engineering*. 82, pp. 14-24. 2015.
<https://doi.org/10.1016/j.ijimpeng.2015.04.008>
- [31] Fiedler, T., Taherishargh, M., Krstulovic-Opara, L., Vesjenjak, M. "Dynamic compressive loading of expanded perlite/aluminum syntactic foam." *Materials Science and Engineering: A*. 626, pp. 296–304. 2015.
<https://doi.org/10.1016/j.msea.2014.12.032>
- [32] Orbulov, I. N., Ginzler, J. "Compressive characteristics of metal matrix syntactic foams." *Composites Part A: Applied Science and Manufacturing*. 43(4), pp. 553–61. 2012.
<https://doi.org/10.1016/j.compositesa.2012.01.008>
- [33] Zhang, B., Lin, Y., Li, S., Zhai, D., Wu, G. "Quasi-static and high strain rates compressive behavior of aluminum matrix syntactic foams." *Composites Part B: Engineering*. 98, pp. 288–296. 2016.
<https://doi.org/10.1016/j.compositesb.2016.05.034>
- [34] Jaeger, H. M., Nagel, S. R. "Physics of the granular state." *Science*. 255(5051), pp. 1523-1531. 1992.
<https://doi.org/10.1126/science.255.5051.1523>
- [35] Torquato, S., Truskett, T. M., Debenedetti, P. G. "Is random close packing of spheres well defined?" *Physical Review Letters*. 84(10), pp. 2064–2067. 2000.
<https://doi.org/10.1103/PhysRevLett.84.2064>
- [36] Alvandi-Tabrizi, Y., Whisler, D. A., Kim, H., Rabiei, A. "High strain rate behavior of composite metal foams." *Materials Science and Engineering: A*. 631, pp. 248–257. 2015.
<https://doi.org/10.1016/j.msea.2015.02.027>